Supplementary Material

1. Supplementary materials and methods

Animal procedures

All animal procedures were approved by the Institutional Animal Care & Use Committee of the University of Michigan (PRO00006176) and performed in accordance with the institutional guidelines. Eight weeks-old male C57BL/6J and apoE$^{-/-}$ mice (B6.129P2-Apoe^{tm1Unc}/J, Stock No.: 002052) were obtained from Jackson Laboratories. Mice were subjected to subcutaneous implantation of osmotic minipumps for delivery of polyethylenglycol (PEG)-solvated OA-NO_2 or oleic acid (OA) at an infusion rate of 5 or 8 mg/kg/day as previously described (1-3). ApoE$^{-/-}$ mice were fed chow-diet (CD, 13% of calories from fat, LabDiet 5L0D) or western-diet (42% of calories from fat and 0.2% cholesterol by weight, Envigo TD.88137, Supplemental Tables 1 and 2) for 8 weeks. Control C57BL/6J mice for the NASH experimental design were fed a standard chow diet (CD) for 24 weeks and implanted with PEG-loaded osmotic minipumps at the time of randomization (week 12, Figure 1a). NASH-diet regime consists in saturated fat, trans-fat, fructose and cholesterol feeding for 24 weeks (Supplementary Tables 3 and 4, 40% of calories from fat, Research Diets D17010103). All mice were maintained on a 12-hour light/dark cycle and had *ad libitum* access to food and water.

Non-invasive *in vivo* imaging for dual analysis of hepatic steatosis and fibrosis

Hepatic lipid and collagen contents were quantitatively determined *in vivo* by photoacoustic imaging using a photoacoustic-ultrasound (PA-US) dual modality system (4). During the procedure, mice were anesthetized with ketamine (100 mg/kg) and xylazine (10mg/kg) injection. The imaging geometry is identical to that used in our previous study (5). Briefly, a CL15-7 ultrasound (US) transducer array was accurately positioned by a 3-dimensional translation stage. Livers were first located in subcostal oblique plane in the US modality alone. Optical illumination at 1220 and 1370 nm, targeting liver lipid and collagen content respectively, were turned on for parallel US and PA imaging. The PA images were reconstructed using delay-and-sum approach. The contours of the livers were manually delineated and co-registered to the PA images. The PA signal intensities within the liver regions in each frame were averaged. Averaged PA intensities in

the neighboring 10 frames were averaged again to produce a single quantitative measurement at each wavelength.

Histology

Histology processing was performed by the In Vivo Animal Core (IVAC) histology laboratory within the Unit for Laboratory Animal Medicine at Michigan Medicine. Formalin-fixed tissues were processed through graded alcohols and cleared with xylene followed by infiltration with molten paraffin using an automated VIP5 or VIP6 tissue processor (TissueTek, Sakura-Americas, Torrance, CA). Following paraffin embedding using a Histostar Embedding Station (ThermoScientific, Hanover Park, IL), tissues were then sectioned on a M 355S rotary microtome (ThermoFisher Scientific, Hanover Park, IL) at 4 μm thickness and mounted on glass slides. Following deparaffinization and hydration with xylene and graded alcohols, slides were stained with Harris hematoxylin (ThermoFisher Scientific, Cat# 842), differentiated with Clarifier (ThermoScientific, Cat#7401), blued with bluing reagent (ThermoFisher Scientific, Cat#7301), stained with eosin Y, alcoholic (ThermoFisher Scientific, Cat# 832), then dehydrated and cleared through graded alcohols and xylene and coverslipped with Micromount (Leica cat# 3801731, Buffalo Grove, IL) using a Leica CV5030 automatic coverslipper.

PicroSirius Red Staining

Following deparaffinization and hydration with xylene and graded alcohols, slides were treated with 0.2 Phosphomolybdic Acid (Rowley Biochemical Inc., F-357-1) for 3 min, directly transferred to 0.1% Sirius Red saturated in picric acid (Rowley Biochemical Inc., F-357-2) for 90 min, then again directly transferred to 0.01N Hydrochloric Acid for 3 min. Slides were dehydrated and cleared through graded alcohols and xylene and coverslipped with Micromount (Leica cat# 3801731, Buffalo Grove, IL) using a Leica CV5030 automatic coverslipper.

Frozen Section Processing and Oil Red O Staining

Formalin-fixed liver samples were cryoprotected in 20% sucrose at 4 degrees overnight, blotted, then liquid nitrogen-snap frozen in O.C.T. Compound (Tissue-Tek, Cat #4583) and stored at -80 until ready for cryosectioning. Prior to sectioning, frozen blocks were brought up to about -20 degrees, then sectioned at 5 microns on a Cryotome SME (Thermo-Shandon, Cat# 77200227). Slides were stored at -80 degrees until stained. Prior to staining, liver slides were removed from -80 and thawed to room temperature for 30 min. Slides were post-fixed in 10% Neutral Buffered

Formalin for 10 min, rinsed in deionized water, and stained in working Oil Red O-isopropanol stain (Rowley Biochemical Inc., H-503-1B) for 10 min. Following three changes of deionized water, slides were nuclear counterstained in Harris Hematoxylin and mounted in Aqua-Mount (Lerner Laboratories, Cat# 13800) aqueous mounting media

Immunohistochemistry (IHC) Staining

Rehydrated slides were subjected to heat-induced antigen retrieval in Diva Decloaking Buffer, ph 6.2 (Biocare Medical, Cat# DV2004) using a Decloaking Chamber pressure cooker (Biocare Medical, Cat#DC2002). Immunohistochemical staining was performed on a IntelliPATH FLX automated immunohistochemical stainer (Biocare Medical, Cat# IPS0001US) and included blocking for endogenous peroxidases and non-specific binding, detection using a horseradish peroxidase biotin-free polymer based commercial detection system, disclosure with diaminobenzidine chromogen, and nuclear counterstaining with hematoxylin.

Specific to alpha smooth muscle Actin (Abcam, Cat# ab5694), the rabbit polyclonal primary antibody was diluted to 1:1800 in DaVinci Diluent (Biocare Medical, Cat# PD900) and incubated for 60 min followed by detection using Rabbit on Rodent HRP-Polymer, Biocare Medical, Cat# RMR622) for 30 min.

Specific to F4/80, (Bio-Rad ABD Serotec, Cat# MCA497), the rat monoclonal primary antibody (clone CI:A3-1) was diluted to 1:400 in DaVinci Diluent (Biocare Medical, Cat# PD900) and incubated for 60 min followed by detection using Rat-on-Mouse HRP-Polymer, (Biocare Medical, Cat# RT517) 2-step probe-polymer incubation for 10 and 30 min respectively.

Liver steatosis, lobular inflammation and fibrosis scoring

H&E and Sirius red staining were used to score liver steatosis, lobular inflammation and fibrosis as previously described (6). Briefly, steatosis was scored from 0-3 (0: <5% steatosis; 1: 5-33%; 2: 34-66%; 3: >67%). Hepatocyte ballooning was scored from 0-2 (0: normal hepatocytes, 1: normal-sized hepatocytes with pale cytoplasm, 2: pale and enlarged hepatocytes, at least 2-fold than normal hepatocytes). Lobular inflammation was scored from 0-2 based on foci of inflammation counted at 20X (0: none, 1: ≤ 2 foci; 2: >2 foci). NAFLD activity score was calculated as the sum of steatosis, hepatocyte ballooning and lobular inflammation scores. Fibrosis was scored from 0-4 (0: no fibrosis; 1: perisinusoidal or portal fibrosis; 2: perisinusoidal and portal fibrosis; 3: bridging fibrosis; 4: cirrhosis).

Mouse comprehensive laboratory animal monitoring system (CLAMS) and body composition analysis

Oxygen consumption (VO_2), carbon dioxide production (VCO_2) and motor activity were measured using the Comprehensive Laboratory Monitoring System (CLAMS, Columbus Instruments), an integrated open-circuit calorimeter equipped with an optical beam activity monitoring device. Mice were weighed each time before the measurements and individually placed into the sealed chambers (7.9" x 4" x 5") with free access to food and water. The study was carried out in an experimentation room set at 20-23°C with 12-12 hours (6:00PM~6:00AM) dark-light cycles. The measurements were carried out continuously for 48 h. During this time, animals were provided with food and water through the equipped feeding and drinking devices located inside the chamber. VO_2 and VCO_2 in each chamber were sampled sequentially for 5s in 10 min intervals and the motor activity was recorded every second in X and Z dimensions. The air flow rate through the chambers was adjusted at the level to keep the oxygen differential around 0.3% at resting conditions. Respiratory exchange ratio (RER), was calculated as VCO_2/VO_2. Total energy expenditure, carbohydrate oxidation, and fatty acid oxidation were calculated respectively based on the values of VO_2, VCO_2, and the protein breakdown.

Body fat, lean mass, and free fluid were measured using a nuclear magnetic resonance (NMR)-based analyzer (Minispec LF90II; Bruker Optics, Billerica, MA). Conscious mice were placed individually into the measuring tube with a minimum restrain. The machine is daily checked using a reference sample as recommended by the manufacture.

RNA-sequencing analysis

Total RNA of 12 liver samples were extracted with Trizol reagent and cleaned up with Qiagen clean-up kit (Cat# 74204). Libraries were prepared with Roche KAPA mRNA HyperPrep Kit (KK8581) following the manufacturer's protocol and being paired-end sequenced (2 x 76bp) on Illumina HiSeq 4000 platform. Quality control for the raw sequence reads were analyzed with FASTQC (https://www.bioinformatics.babraham.ac.uk/projects/fastqc/). Adaptors and low-quality reads were trimmed by Trimmomatic v0.35 (7). The trimmed high-quality reads were mapped to the mouse genome NCBI GRCm38 using HISAT2 v2.1.0 (8). The resulting SAM files were sorted, indexed, and converted to BAM files using Samtools v1.2 (9). The total number of reads that were mapped to gene were quantified using HTSeq-counts v0.6.0 (10) under the union model with NCBI GRCm38 genome annotations. The differentially expressed genes (DEGs) between groups were analyzed using DESeq2 (11). Genes with FDR p value less than 0.05 and absolute value of

fold change larger than 2 were considered as significant DEGs. The data discussed in this publication have been deposited in NCBI's Gene Expression Omnibus (12) and are accessible through GEO Series accession number GSE126204 www.ncbi.nlm.nih.gov/geo/query/acc.cgi?acc=GSE126204

Ingenuity pathway analysis (IPA)

IPA (Ingenuity Systems, Redwood City, CA, USA) analysis was performed to identify signaling pathways that are significantly enriched in DEGs. Up- and down-regulated DEGs were analyzed separately. The significance level of enrichment was determined by right-tailed Fisher's exact test.

Hepatic lipid extraction

Livers were rapidly removed from the euthanized mice and kept at -80°C. Frozen liver samples (approximately 100 mg) were homogenized in PBS and centrifuged (14,000 RPM, 20 min). The supernatants were collected and analyzed for protein content by the Bio-Rad Bradford assay. To assess liver lipid composition, lipids were extracted from the supernatants using hexane (≥99%, 32293, Sigma-Aldrich) and isopropanol (≥99.5%, A426-4, Fisher Scientific) at a 3:2 ratio (*v:v*), and the hexane phase was left for evaporation for 48 h. The amount of liver triglycerides (TG) or cholesterol was determined spectrophotometrically using commercially available kits (Wako Chemicals). Data were normalized to protein levels and presented as µg TG or cholesterol / mg protein.

Measurement of collagen content of liver tissue

Collagen content in the livers was evaluated by measuring the hydroxyproline level in the livers using the Hydroxyproline Colorimetric Assay Kit (K555100) from BioVision. Briefly, liver tissue was homogenized in water and samples were hydrolyzed by incubation with 10N hydrochloric acid at 120°C for 3 hours. Liver hydrolysates were oxidized using chloramine-T, followed by incubation with Ehrlich's perchloric acid reagent for color development. Absorbance was measured at 560 nm, and hydroxyproline quantities were calculated by reference to standards processed in parallel.

Plasma lipid profile and glucose

Plasma levels of total cholesterol (TC) and TG were determined spectrophotometrically using a commercially available kit (Wako Chemicals). Low-density lipoprotein cholesterol (LDL) and high-

density lipoprotein (HDL) levels were measured with a Cobas Mira chemistry analyzer (Roche Diagnostics) at the Chemistry Laboratory of the Michigan Diabetes Research Center (MDRC) using manufacturer-provided assay reagents and protocols. Blood glucose-meter and test strips (NDC: 0193-7308-50, Contour Next) levels were used to measure plasma glucose levels.

Plasma liver panel

Clinical chemistry assays for alanine aminotransferase (ALT), aspartate aminotransferase (AST), alkaline phosphatase (ALP), and albumin (ALB) were performed by the In Vivo Animal Core (IVAC, University of Michigan) on a Liasys 330 chemistry analyzer (AMS Diagnostics) using manufacturer-provided assay reagents and protocols. Quality control for operation of the analyzer is monitored daily using manufacturer-provided control samples. Multiplex Mouse Cytokine/Chemokine Bead Panel (MCYTOMAG-70K, Millipore) for detection of plasma levels of Mcp-1 and IL-6 on a Luminex 200 platform (Luminex).

RNA expression and biochemical analyses.

Total RNA from mouse liver samples was extracted using QIAGEN's RNeasy kits (QIAGEN). RNA was reverse-transcribed into cDNA with SuperScript III and random primers (Invitrogen). Specific transcript levels were assessed by a real-time PCR system (Bio-Rad) using iQ SYBR Green Supermix (Bio-Rad) and the ΔΔCt threshold cycle method of normalization. Gene expression levels were normalized to glyceraldehyde 3-phosphate dehydrogenase (GAPDH). Primer pairs used for qPCR were obtained from Integrated DNA Technologies and are listed in Supplemental Table 5.

Isolation of primary hepatocytes

C57BL/6 mice were anesthetized with ketamine and xylazine and opened through the peritoneal cavity to expose the inferior vena cava and hepatic portal vein. The suprahepatic inferior vena cava was ligated and the infrahepatic inferior vena cava was cannulated for in situ perfusion with pre-warmed (37^{o}C) Liver Perfusion Medium (Gibco). Livers were then perfused with Liver Digest Medium (Gibco). After collagenase/dispase perfusion, livers were transferred to 15ml cold (4^{o}C) L-15 medium (Gibco) and passed through a 100μm cell strainer to obtain a single cell dispersion. Cells were washed with cold (4^{o}C) Hepatocyte Wash Medium (Gibco). Exclusion of non-parenchymal cells was achieved after resuspending the cells in 15% Nycodenz to form a gradient

after centrifugation at 500g. Purified hepatocytes were cultured in pre-coated 12-well plates (Collagen I, Gibco).

Human hepatic stellate cells and HepG2 cells

Human hepatic stellate cells (HSCs) were obtained from ScienCell (Catalog # 5300) and HepG2 human hepatoma cell line was obtained from the American Type Culture Collection (ATCC). Cells were cultured at 37˚C and 5% CO_2 in Dulbecco's Modified Eagle Medium (DMEM, Gibco) supplemented with 10% fetal bovine serum (FBS, Sigma-Aldrich) and 1% Penicillin-Streptomycin (Pen-Strep, Gibco). 70% confluent HSCs or HepG2 cells were used for all experiments. Cell treatments with palmitic acid (PA, Sigma-Aldrich), TGF-β (Sigma-Aldrich), and OA, OA-NO_2 or ethanol (vehicle control) were conducted in reduced-FBS DMEM (1%).

Western blot analysis

Cells and mouse tissues were lysed in T-PER, Tissue Protein Extraction Reagent (Thermo Scientific) supplemented with a protease inhibitor cocktail (Roche Applied Science). Protein extracts were resolved in 10% SDS–PAGE gels and transferred to PVDF membranes (Bio-Rad). After blocking in TBST containing 5% non-fat dry milk at room temperature for 1 hour, the PVDF membranes were immunoblotted with primary antibodies at 4°C overnight. The following antibodies were used: SREBP-1 (2A4) (Santa Cruz Biotechnology, sc-13551; 1:1000); CTGF (E-5) (Santa Cruz Biotechnology, sc-365970; 1:500), Anti-Actin, α-Smooth Muscle (Clone 1A4 Sigma, 1:1000); phospho-Smad2 (Ser245/250/255) (Cell Signaling, #3104S; 1:1000); Smad2 (D43B4) XP® Rabbit mAb (Cell Signaling, #5339S; 1:1000); GAPDH (Santa Cruz Biotechnology; 1:1000). The membranes were washed by TBST before incubated with IRDye-conjugated secondary antibodies (1:5000, LI-COR Biosciences) at room temperature for 1 hour. Western blots were scanned and quantified using an Odyssey Infrared Imaging System (LI-COR Biosciences, version 2.1).

Cellular lipid extraction

Following cell treatments, cellular lipids were extracted with hexane:isopropanol (3:2,*v:v*), and the hexane phase was left for evaporation for 48 h. The remaining cells in the plates were dissolved in 0.1 M NaOH and an aliquot was taken for measurement of cellular protein using the Bradford protein assay (Bio-Rad). Cellular TG content was determined spectrophotometrically using a commercially available kit (Wako Chemicals). TG data were normalized to cellular protein levels.

Cellular TG biosynthesis rate

Cellular TG biosynthesis was assayed after incubation of HepG2 cells for 3 h at 37°C with [^{3}H]-acetate (3.3 µCi/ml, ART 0202, American Radiolabeled Chemicals) in serum-free medium supplemented with 0.1% BSA. Cellular lipids were extracted as described above and lipids were then separated by thin layer chromatography (TLC) on silica gel plates (60 F254, M1057150001, Fisher Scientific) and developed in hexane / ether (≥99.9%, 309966, Sigma-Alrich) / acetic acid (≥99.7%, A38-212, Fisher Scientific) at a 130:30:1.5 ratio (*v:v:v*). TG spots were visualized by iodine vapor (by using an appropriate standard for identification) and [^{3}H]-labels were counted by a Tri-Carb 2810TR liquid scintillation analyzer (PerkinElmer). Data were normalized to protein levels and presented as count per minutes (cpm)/mg cell protein.

Statistical analysis

Statistical analyses were performed using SPSS 24.0 software (SPSS Inc. IBM). Unless indicated otherwise, values are presented as box-plots and whiskers or means ± SEM of at least three independent observations. The number of animals or experiments used for each study is specified for each figure legend. One-way analysis of variance (ANOVA) followed by Bonferroni post hoc test was used for data analysis. Differences were considered statistically significant at $p<0.05$.

2. Supplementary Tables

Table S1: WD macronutrient

Macronutrient	g %	kcal %
Protein	17.3	15.2
Carbohydrate	48.5	42.7
Fat	21.2	42
kcal/gm	4.5	
Cholesterol	0.2	

Table S2: WD components

Ingredient	g
Casein	195.0
DL-methionine	3.0
Sucrose	341.5
Corn starch	150.0
Anhydrous milkfat	210.0
Cholesterol	1.5
Cellulose	50
Mineral Mix	35.0
Vitamin Mix	10.0
Calcium carbonate	4.0
Total	1000.0

Table S3: NASH diet macronutrient

Macronutrient	g %	kcal %
Protein	22	20
Carbohydrate	45	40
Fat	20	40
kcal/gm	4.5	

Table S4: NASH diet components

Ingredient	g
Casein	200.0
L-cystine	3.0
Maltodextrin	100.0
Fructose	200.0
Sucrose	96.0
Cellulose	50.0
Soybean oil	25.0
Primex, Non-transfat	45.0
Corn oil, partially hydrogenated	110.0
Mineral Mix	10.0
DiCalcium Phosphate	13.0
Calcium Carbonate	5.5.
Potassium Citrate	16.5
Mineral Mix	10.0
Choline Bitartrate	2.0
Cholesterol	18.0
Total	904.0

Table S5: Primers used for qPCR

Gene (Mus musculus)		Forward (5'-3')	Reverse (5'-3')
Glyceraldehyde-3-phosphate dehydrogenase	*GAPDH*	CTGCGACTTCAACAGCAACT	GAGTTGGGATAGGGCCTCTC
Sterol regulatory element binding factor 1	*SREBF1c*	TAGAGCATATCCCCCAGGTG	GGTACGGGCCACAAGAAGTA
Sterol regulatory element binding factor 2	*SREBF2*	TGGGAGAGTTCCCTGATTTG	GATAATGGGACCTGGCTGAA
Stearoyl-Coenzyme A desaturase 1	*SCD1*	CGAGGGTTGGTTGTTGATCT	GCCCATGTCTCTGGTGTTTT
Acetyl-Coenzyme A carboxylase alpha	*ACC1*	AATGAACGTGCAATCCGATTTG	ACTCCACATTTGCGTAATTGTTG
Glycerol-3-phosphate acyltransferase	*GPAT1*	ACAGTTGGCACAATAGACGTTT	CCTTCCATTTCAGTGTTGCAGA
Glycerol-3-phosphate acyltransferase	*GPAT1*	GCACATACCCACCAGTTTTGA	AGGATACGCTGTACCTCTTTCT
1-acylglycerol-3-phosphate O-acyltransferase 1	*AGPAT1*	TAAGATGGCCTTCTACAACGGC	CCATACAGGTATTTGACGTGGAG
1-acylglycerol-3-phosphate O-acyltransferase 2	*AGPAT1*	CTTCAAGTACGTGTATGGCCTT	CTGTGAACATTAGCTCACGCT
Monoacylglycerol O-acyltransferase 1	*MOGAT1*	TCCCGTTGTTCCGAGAATATCT	TGCTCAGCACATGAGACAAAC
Monoacylglycerol O-acyltransferase 2	*MOGAT2*	CGGGCTTTACCTCGCTTTTC	CCCAGACATGATGTAATCTCGGA
Diacylglycerol O-Acyltransferase 1	DGAT1	GCTTCTGCAGTTTGGAGACC	CTCATGGAAGAAGGCTGAGG
Diacylglycerol O-Acyltransferase 2	DGAT2	TCCAGCTGGTGAAGACACAC	GATGCCTCCAGACATCAGGT
Peroxisome proliferator activated receptor alpha	*PPARα*	AACATCGAGTGTCGAATATGTGG	CCGAATAGTTCGCCGAAAGAA
Protein kinase, AMP-activated, alpha 1 catalytic subunit	*AMPK1*	GTCAAAGCCGACCCAATGATA	CGTACACGCAAATAATAGGGGTT
Carnitine palmitoyltransferase 1a, liver	*CPT1a*	AGATCAATCGGACCCTAGACAC	CAGCGAGTAGCGCATAGTCA
Mitochondrial carnitine/acylcarnitine translocase	*CACT*	CAACCACCAAGTTTGTCTGGA	CCCTCTCTCATAAGAGTCTTCCG
Acyl-Coenzyme A oxidase 1, palmitoyl	*ACOX1*	CCGCCACCTTCAATCCAGAG	CAAGTTCTCGATTTCTCGACGG
Acyl-Coenzyme A dehydrogenase, medium chain	*ACADm*	AGGGTTTAGTTTTGAGTTGACGG	CCCCGCTTTTGTCATATTCCG
Uncoupling protein 2	*UCP2*	ATGGTTGGTTTCAAGGCCACA	TTGGCGGTATCCAGAGGGAA
Tumor necrosis factor	*TNFα*	CTGTGAAGGGAATGGGTGTT	GGTCACTGTCCCAGCATCTT
Interleukin 1 beta	*IL-1β*	GGGCCTCAAAGGAAAGAATC	TACCAGTTGGGGAACTCTGC
Interleukin 6	*IL-6*	TAGTCCTTCCTACCCCAATTTCC	TTGGTCCTTAGCCACTCCTTC
C-C motif chemokine ligand 2	*Ccl2*	TTAAAAACCTGGATCGGAACCAA	GCATTAGCTTCAGATTTACGGGT
C-C motif chemokine ligand 5	*Ccl5*	GCTTTGCAGCTCTTCCTCAT	GTCACCATCCTTTTGCCAGT
Transforming growth factor, beta 1	*TGFβ1*	TGCGCTTGCAGAGATTAAAA	CTGCCGTACAACTCCAGTGA
Connective tissue growth factor	*CTGF*	AGCAGCTGGGAGAACTGTGT	GCTGCTTTGGAAGGACTCAC
Collagen, type I, alpha 1	*COL1A1*	TGAACGTGACCAAAAACCAA	GCAGAAAAGGCAGCATTAGG
Collagen, type I, alpha 2	*COL1A2*	AGGCAGGTCTGGGCTTTATT	CGTATCCACAAAGCTGAGCA
Tissue inhibitor of metalloproteinase 1	*TIMP1*	ATTCAAGGCTGTGGGAAATG	CTCAGAGTACGCCAGGGAAC
Actin, alpha 2	*ACTA2*	CTGACAGAGGCACCACTGAA	CATCTCCAGAGTCCAGCACA
Serine (or cysteine) peptidase inhibitor, clade E, member 1	*SerpinE1*	GTAGCACAGGCACTGCAAAA	ATCACTTGGCCCATGAAGAG
Triggering Receptor Expressed On Myeloid Cells 2	*TREM2*	AGGAATCAAGAGACCTCCTTCC	CAGTGAGGATCTGAAGTTGGTG
Toll Like Receptor 2	*TLR2*	CGGCTGCAAGAGCTCTATATTT	GAGTCTCCAGTTTGGGAAAAGA
Toll Like Receptor 4	*TLR4*	CAGCACTCTTGATTGCAGTTTC	CATTCACCAAGAACTGCTTCTG

Table S5: Primers used for qPCR (cont)

Gene (Mus musculus)		Forward (5'-3')	Reverse (5'-3')
Toll Like Receptor 1	*TLR1*	CAGCACTCTTGATTGCAGTTTC	CATTCACCAAGAACTGCTTCTG
Intercellular Adhesion Molecule 1	*ICAM1*	CAGGAGGAGGCCATAAAACTC	TCTGTGACAGCCAGAGGAAGT
Vascular Cell Adhesion Molecule 1	*VCAM1*	ATTGGGAGAGACAAAGCAGAAG	CTCCAAGAAAAAGAAGGGGAGT
Epithelial Cadherin	*E-Cadherin*	ATCCTTCATGTGAGAGTGGAGAA	CGAGCGGTATAAGATGTGATTTC
Hydroxysteroid 17-Beta Dehydrogenase 10	*HSD17B10*	GGCCGTATAGATGTGGCTGT	CTCCCTGGTCTGGTTCATTC
Acyl-CoA Synthetase Long Chain Family Member 1	*ACSL1*	CAAGGTCAATGAGGACACGA	TCTTCTTGTTGGTGGCACTG
Enoyl-CoA Delta Isomerase 1	*ECI1*	CTGGACTTGCTGGAGATGTATG	CAGCCATAACCCTGTAGTCACA
PPARgamma Coactivator 1alpha	*PPARGC1A*	ATCACGTTCAAGGTCACCCTAC	TTCTGCTTCTGCCTCTCTCTCT

3. Supplementary Figures

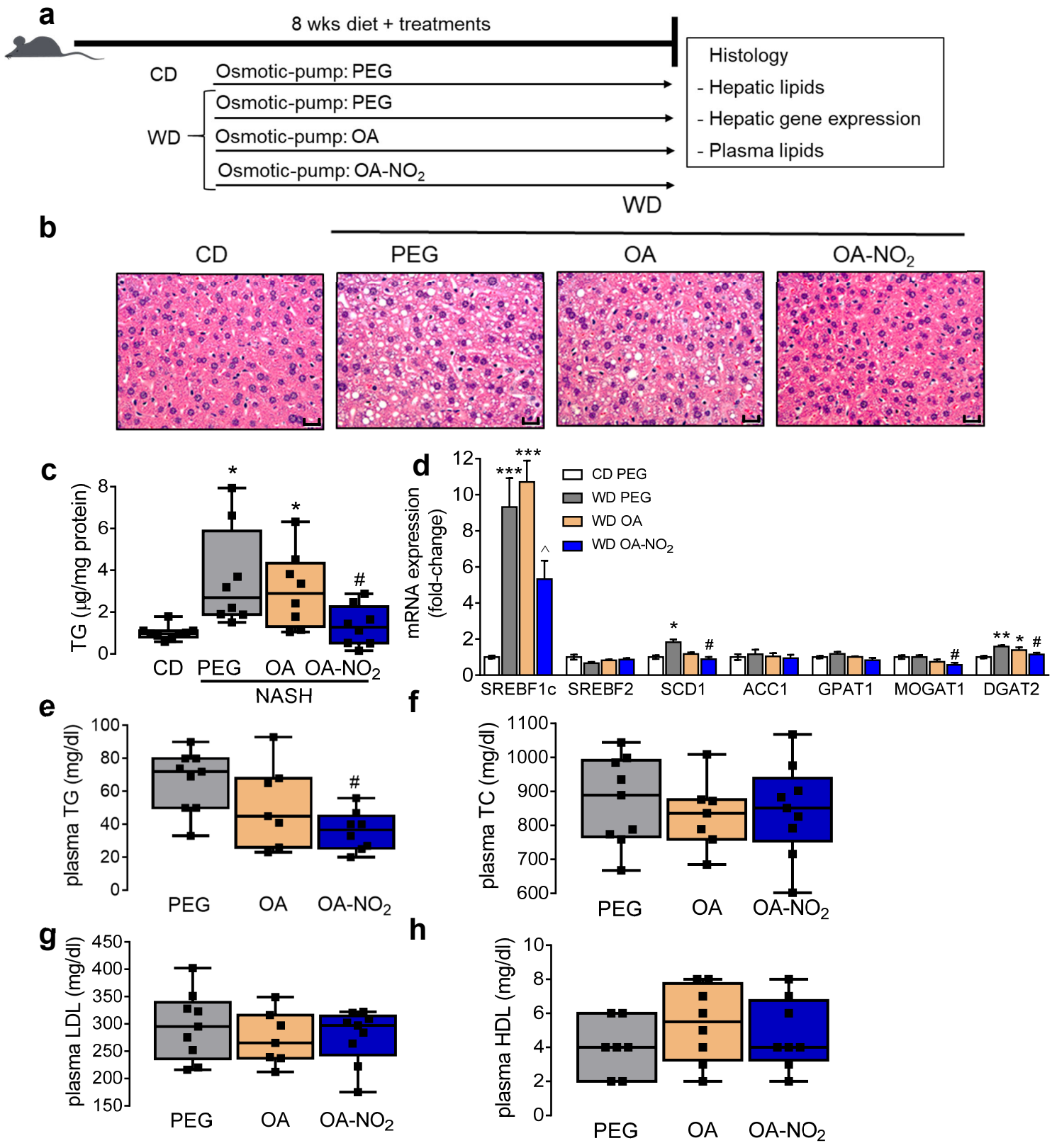

Supplementary Figure 1: **OA-NO$_2$ prevents WD-induced hepatic steatosis in apoE$^{-/-}$ mice**

(a) Experimental design: apoE$^{-/-}$ mice were fed CD or WD and administrated OA-NO$_2$ (8 mg/kg/d)

by subcutaneously implanted osmotic minipumps. Mice fed CD and administrated PEG (vehicle) as well as mice fed WD and administrated PEG or non-nitrated OA (8 mg/kg/d) were served as controls (n=8 mice per group). (b) Histological H&E staining. Size bars= 50µm. (c) Hepatic TG content determined following tissue lipid extraction. (d) qPCR analysis of hepatic expression of genes regulating lipogenesis. Fasting plasma levels of (e) TG, (f) TC, (g) LDL, and (h) HDL. *p <0.05 vs. CD PEG; $^{\#}$p <0.05 vs. WD PEG; $^{\wedge}$p <0.05 vs. WD OA.

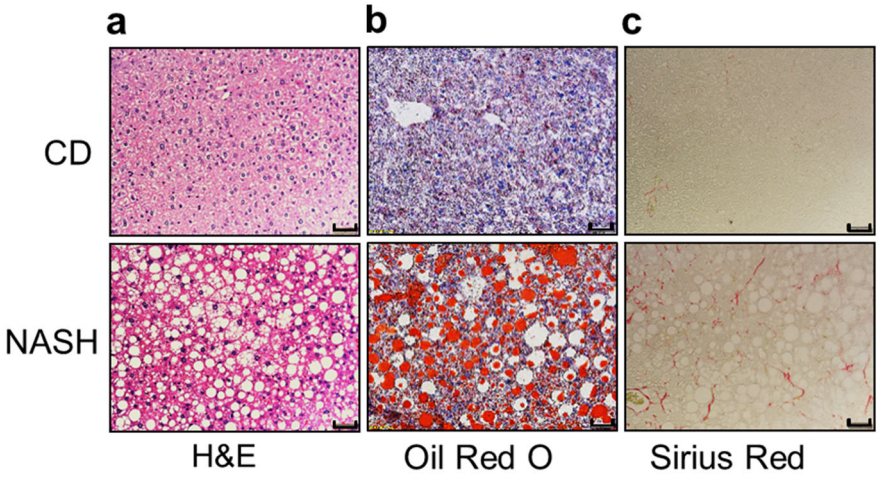

Supplementary Figure 2: Hepatic pathology verification after *in vivo* diagnosis. Established liver steatosis and fibrosis were confirmed in a subpopulation (n=3) analyzed after 12 weeks of NASH diet in C57BL-6J mice and verified by histological analysis as follows: (a) H&E to confirm enlarged hepatocyte ballooning, (b) Oil Red O staining for lipid content, and (c) Sirius Red staining for collagen content. Size bars= 50µm.

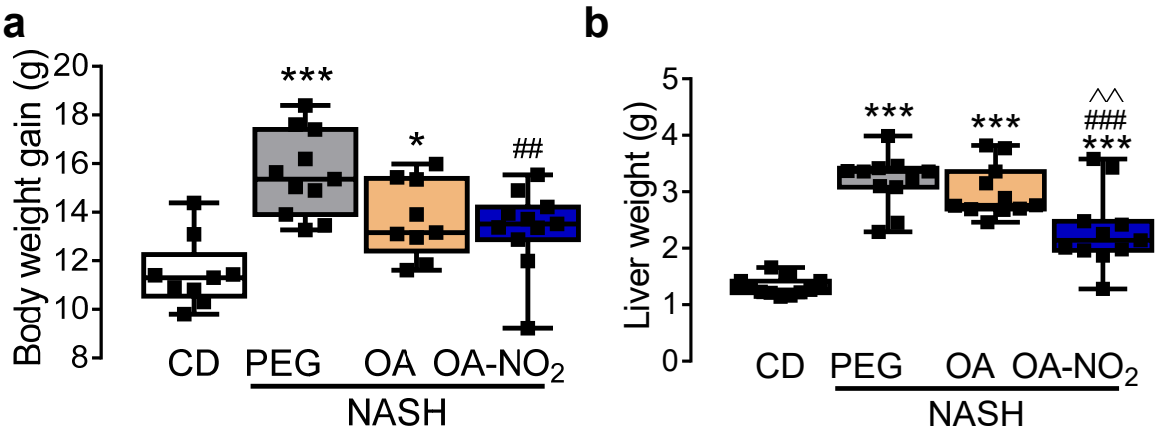

Supplementary Figure 3: OA-NO_2 reduces hepatomegaly during NASH development. (A) Body weight gain from each experimental group since the initiation of NASH-diet feeding. (B) Liver weight at end-point analysis. Data is shown as box and whiskers for the median and minimum to maximum values. *$p < 0.05$, ***$p < 0.001$ vs. CD; $^{\#\#}p < 0.01$, $^{\#\#\#}p < 0.001$ vs. NASH PEG; $^{\wedge\wedge}p < 0.01$ NASH OA.

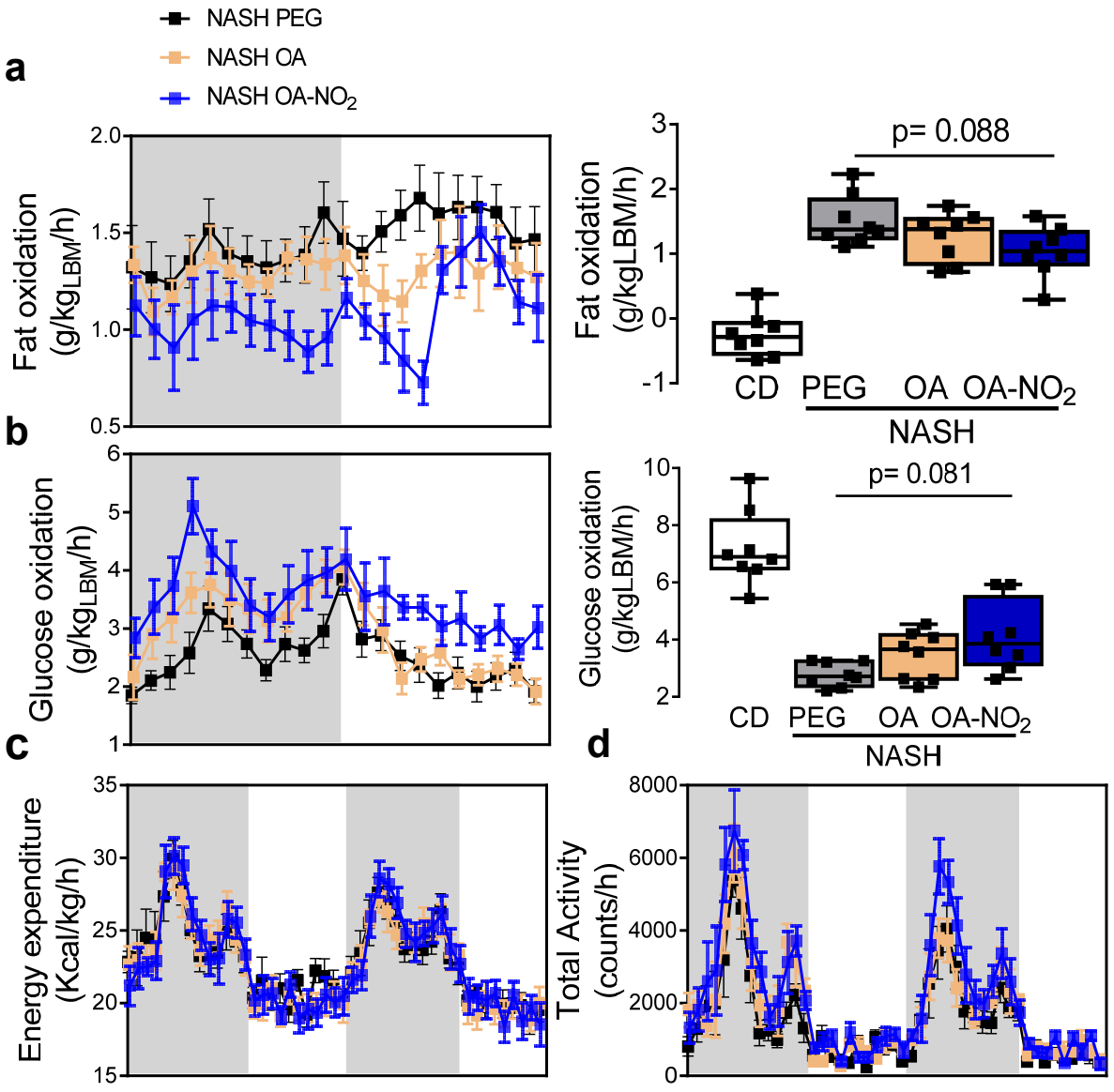

Supplementary Figure 4: OA-NO$_2$ treatment during NASH-diet feeding improves body composition and promotes a metabolic phenotype similar to CD feeding. At week 23 (11 weeks of PEG, OA or OA-NO$_2$ administration), NMR-based body composition analysis and CLAMS were conducted (n=8). (a) Fat oxidation over a 24 h dark/light period. (b) Glucose oxidation over a 24 h dark/light period. There were no differences in total energy expenditure (c) or total activity (d) over a 48h period of the CLAMS analysis between the groups (n=8).

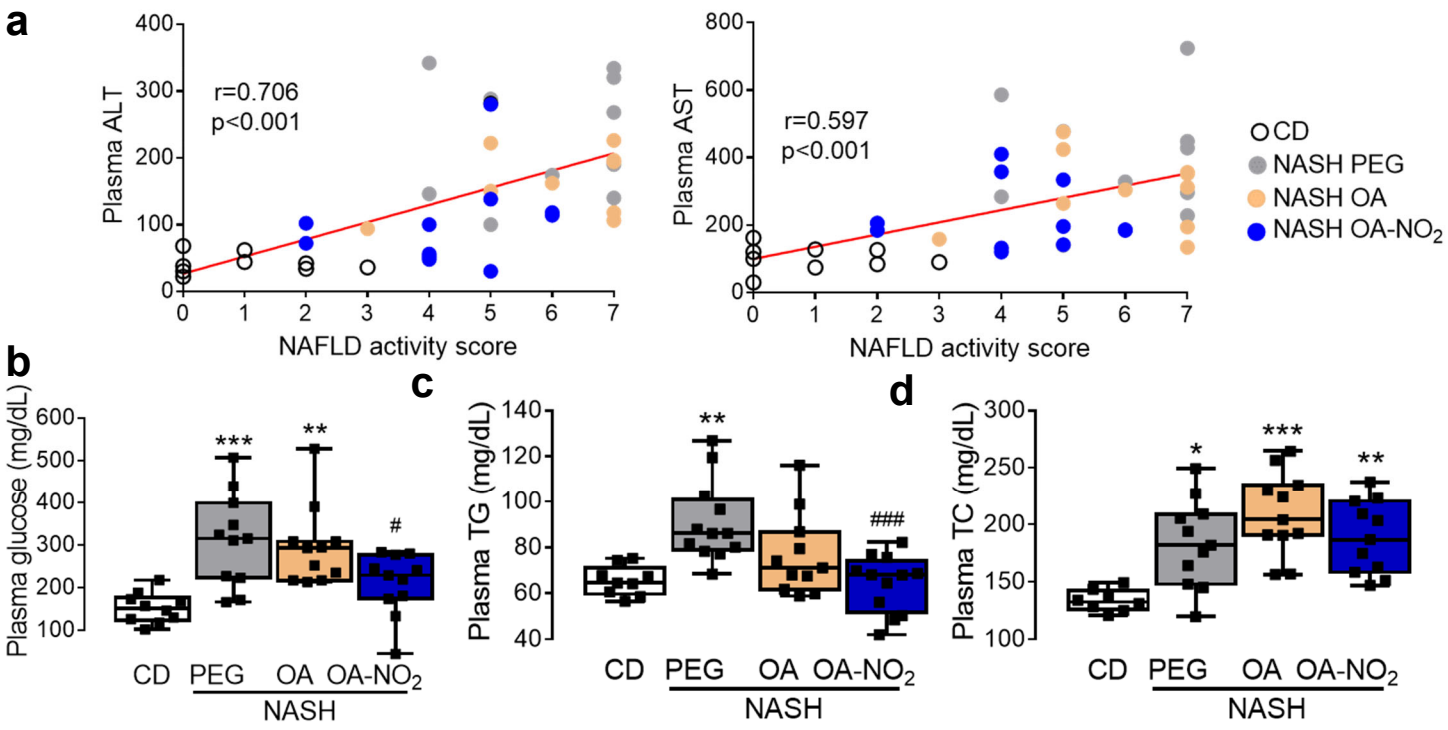

Supplementary Figure 5: Plasma hepatic liver damage analysis, fasting glucose, triglycerides (TG) and total cholesterol (TC) levels. (a) Spearman's correlation analyses between NAFLD activity score and plasma levels of ALT and AST. Exact values of each individual animal from OA-NO_2, OA or PEG after NASH-diet feeding is indicated compared to chow diet controls (CD) and grouped in colors. (b) Fasting glucose levels, (c) total triglycerides (TG) and (d) total cholesterol (TC). Data is shown as box and whiskers for the median and minimum to maximum values, n=9-10. *p<0.05, **p<0.01, ***p<0.001 vs CD PEG; $^{\#}$p<0.05, $^{\#\#\#}$p<0.001 vs. NASH PEG.

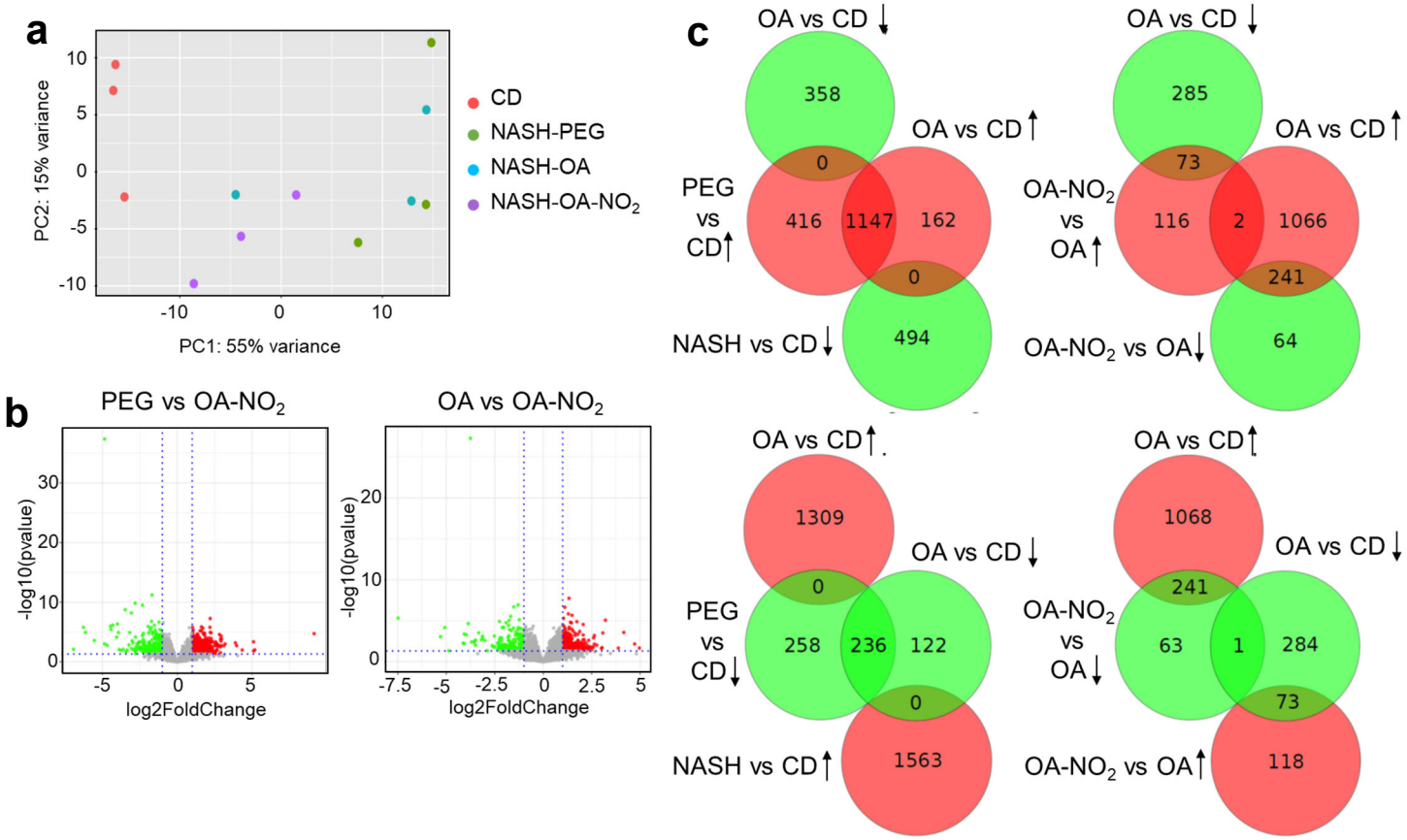

Supplementary Figure 6: a). Principal component analysis (PCA) plot of the transcription profiling of 12 samples. (b) Volcano plots of NASH PEG vs. OA-NO_2 and OA vs. OA-NO_2. X axis represents the log2FoldChange of each gene, and the Y axis represents the -log10 transformation of p values. Genes with p value less than 0.05 and log2FoldChange larger than 1 were considered as significant DEGs. Up-regulated DEGs were in red, down-regulated DEGs were in green, and the non-significant genes were in grey. (c) Venn diagrams depicting multiple comparison between all experimental groups.

a

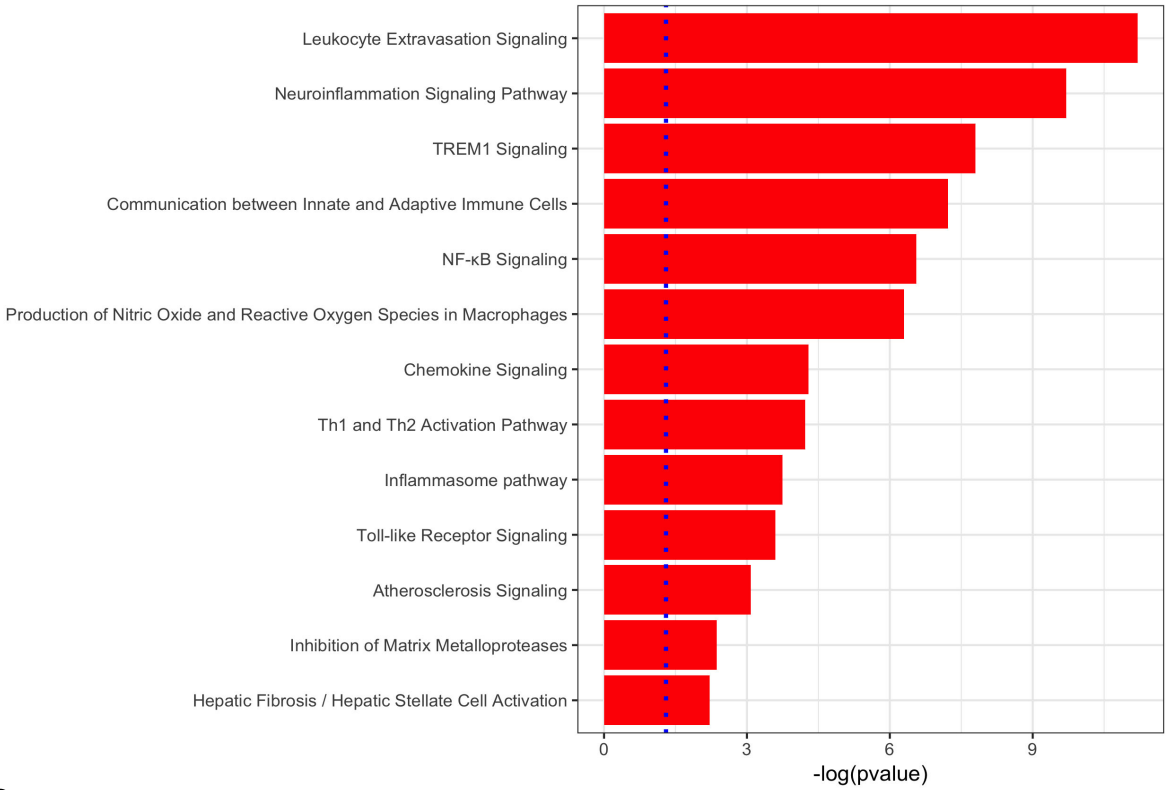

b

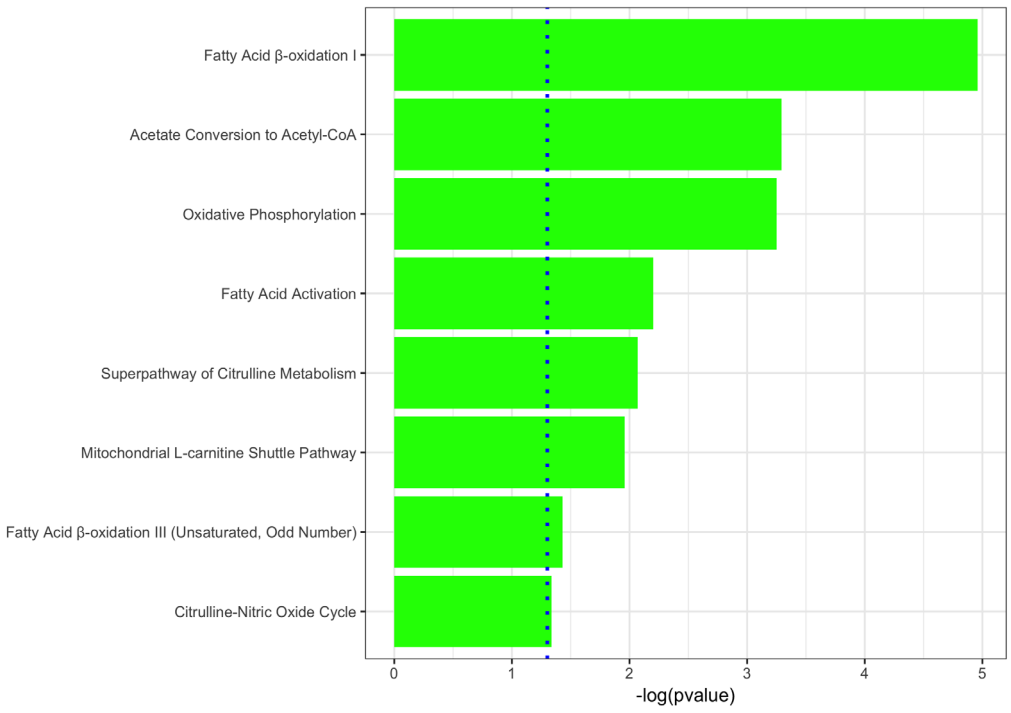

Supplementary Figure 7: Ingenuity pathway analysis. Pathways that are enriched in the up-regulated DEGs were plotted in red (a), while pathways enriched in the down-regulated DEGs were plotted in green (b).

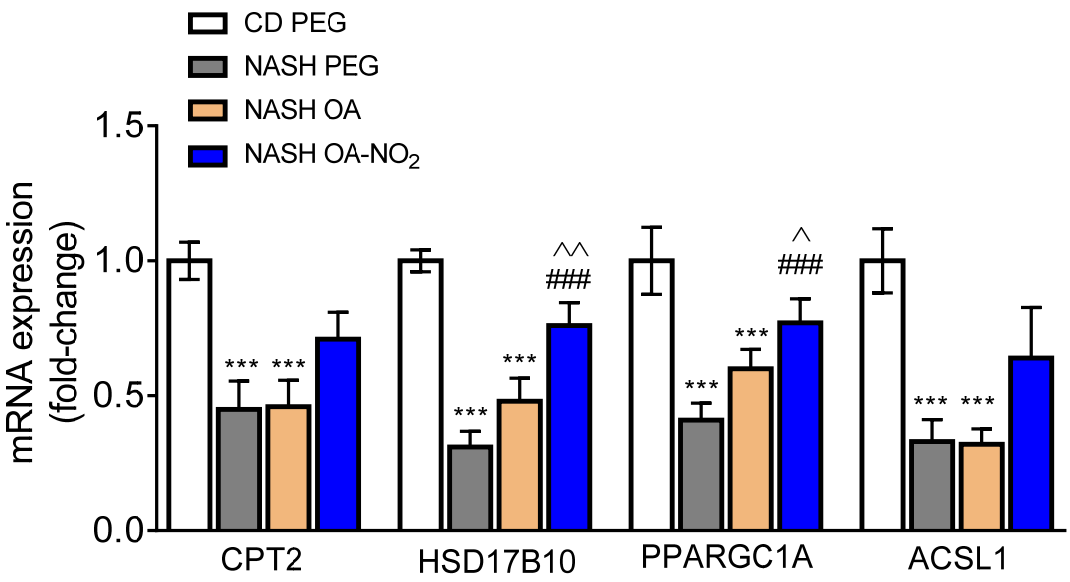

Supplementary Figure 8: qPCR analyses of hepatic expression of genes regulating lipid oxidation identified by RNA-sequencing (n=7-10). Data presented in bars are means ± SEM. ***p <0.001 vs. CD PEG; ###p <0.001 vs. NASH PEG; ^p <0.05, ^^p <0.01 vs. NASH OA.

4. Supplementary References

1. Zhang J, Villacorta L, Chang L, Fan Z, Hamblin M, Zhu T, et al. Nitro-oleic acid inhibits angiotensin II-induced hypertension. Circ Res. 2010;107(4):540-8.
2. Villacorta L, Chang L, Salvatore SR, Ichikawa T, Zhang J, Petrovic-Djergovic D, et al. Electrophilic nitro-fatty acids inhibit vascular inflammation by disrupting LPS-dependent TLR4 signalling in lipid rafts. Cardiovasc Res. 2013;98(1):116-24.
3. Borniquel S, Jansson EA, Cole MP, Freeman BA, Lundberg JO. Nitrated oleic acid up-regulates PPARgamma and attenuates experimental inflammatory bowel disease. Free Radic Biol Med. 2010;48(4):499-505.
4. Yuan J, Xu G, Yu Y, Zhou Y, Carson PL, Wang X, et al. Real-time photoacoustic and ultrasound dual-modality imaging system facilitated with graphics processing unit and code parallel optimization. J Biomed Opt. 2013;18(8):86001.
5. Xu G, Meng ZX, Lin JD, Deng CX, Carson PL, Fowlkes JB, et al. High resolution Physio-chemical Tissue Analysis: Towards Non-invasive In Vivo Biopsy. Sci Rep. 2016;6:16937.

6. Bedossa P, Poitou C, Veyrie N, Bouillot JL, Basdevant A, Paradis V, et al. Histopathological algorithm and scoring system for evaluation of liver lesions in morbidly obese patients. Hepatology. 2012;56(5):1751-9.
7. Bolger AM, Lohse M, Usadel B. Trimmomatic: a flexible trimmer for Illumina sequence data. Bioinformatics. 2014;30(15):2114-20.
8. Kim D, Langmead B, Salzberg SL. HISAT: a fast spliced aligner with low memory requirements. Nat Methods. 2015;12(4):357-60.
9. Li H, Handsaker B, Wysoker A, Fennell T, Ruan J, Homer N, et al. The Sequence Alignment/Map format and SAMtools. Bioinformatics. 2009;25(16):2078-9.
10. Anders S, Pyl PT, Huber W. HTSeq--a Python framework to work with high-throughput sequencing data. Bioinformatics. 2015;31(2):166-9.
11. Love MI, Huber W, Anders S. Moderated estimation of fold change and dispersion for RNA-seq data with DESeq2. Genome Biol. 2014;15(12):550.
12. Edgar R, Domrachev M, Lash AE. Gene Expression Omnibus: NCBI gene expression and hybridization array data repository. Nucleic Acids Res. 2002;30(1):207-10.